INTERNATIONAL JOURNAL FOR NUMERICAL METHODS IN FLUIDS
Int. J. Numer. Meth. Fluids 2006; **51**:1117–1129
Published online 10 February 2006 in Wiley InterScience (www.interscience.wiley.com). DOI: 10.1002/fld.1187

Petrov–Galerkin finite element stabilization for two-phase flows

Michele Giordano*,† and Vinicio Magi‡

Department of Environmental Engineering and Physics, University of Basilicata, Via dell'Ateneo Lucano, Potenza, 85100, Italy

SUMMARY

A finite element model for incompressible laminar two-phase flows is presented. A two-fluid model, describing the laminar non-equilibrium flow of two incompressible phases, is discretized by means of a properly designed streamline upwind Petrov–Galerkin (SUPG) finite element procedure. Such a procedure is consistent with a continuous pressure equation. The design and the implementation of the algorithm are presented together with its validation throughout a comparison with simulations available in the literature. Copyright © 2006 John Wiley & Sons, Ltd.

KEY WORDS: finite element; SUPG; two-fluid model

1. INTRODUCTION

Two-phase flows are encountered in a wide variety of engineering applications ranging from power generation and conversion to biological flows. This leads to a general interest in two-phase flow models [1–3] that may describe the behaviour of these systems. Generally, Eulerian, Lagrangian or mixed approaches are used to represent the phases: depending on the adopted choice, then, next coming matter concerns whether and how to describe the interface. Here, a two-fluid model is used: an Eulerian approach for both phases, and each phase is separately described in terms of two sets of conservation equations. This approach is considered to be appropriate for the most general and detailed description of two-phase flows and represents a fair compromise between the complexity of the model and its suitability to the physics of the problem. This model is obtained through space (or time or space-time or

*Correspondence to: M. Giordano, Department of Environmental Engineering and Physics, University of Basilicata, Via dell'Ateneo Lucano, Potenza, 85100, Italy.
†E-mail: mgiordano@unibas.it
‡E-mail: magi@unibas.it

Contract/grant sponsor: MIUR (Ministero dell'Istruzione, dell'Università e della Ricerca); contract/grant number: PRIN-2003 no. 2003092084_003

Received 2 June 2005
Revised 13 December 2005
Accepted 26 December 2005

ensemble) averaging of the Navier–Stokes equations (NS), and the resulting system represents the combination of two interpenetrating *continua*, where the interaction between the phases are described through *ad hoc* built forces and parameters, and any description of the interface between them is not needed.

In this paper, two-phase steady flows are solved by means of a finite element numerical methodology. The finite element discretization is based on the streamline upwind Petrov–Galerkin (SUPG) method [4–6]. In particular, the system of equations is solved as an advective–diffusive set of equations written in primitive variables and for all of them piecewise linear functions are used, both for the basis and the weighting functions. The main criterium of the proposed discretization is the consistency preservation analogous to single-phase flows. Hence, an extension of the approach used for solving the single-phase NS equations is applied to the two-phase flow equations written subsequently in terms of primitive variables. Since the system of equations is not symmetric, a straightforward direction has not been traced in the SUPG frame, and the idea of maintaining such a consistency greatly helps in the design of the intrinsic time scales. In order to achieve a fair level of stabilization, a discontinuity capturing operator is introduced in order to prevent oscillations in boundary and sharp layer regions.

In the following, the governing equations describing the two-phase flow and the stabilized finite element approach are given. Then, some test cases are presented to validate the proposed methodology. Finally, conclusions are drawn.

2. TWO-PHASE FLOW MODEL

The governing equations of the two-phase flow are presented in this section.

2.1. Basic concepts

The model is an Eulerian–Eulerian one [1], since both phases are treated as *continua*. Moreover, a pressure equilibrium between the phases is assumed, leading to the following relation:

$$p_l = p_g = p \tag{1}$$

where p is the pressure, and the subscripts l and g are referred to as the primary and the secondary phases, respectively.

Since the phases are considered as interpenetrating, non-mixing *continua*, each of them occupies a well-defined volume of space. The volume V_q of the generic phase q is defined by

$$V_q = \int_\Omega \alpha_q \, \mathrm{d}\Omega \tag{2}$$

where α_q is the phasic volume fraction, representing the volume fraction occupied by the phase q in the whole domain Ω. The summation of the phase volumes must recover the whole domain, so that the volume fractions of the phases are coupled by the following relation:

$$\alpha_g + \alpha_l = 1 \tag{3}$$

Equation (3) represents the fundamental constitutive law for the volume fractions.

2.2. Mass conservation

The two-phase flow model must guarantee the conservation of mass.

Referring to the continuity equation of the generic phase q, with the hypothesis of incompressibility, one can write

$$\frac{\partial \alpha_q}{\partial t} + \nabla \cdot (\alpha_q \mathbf{u}_q) = 0 \tag{4}$$

where ρ_q and $\mathbf{u}_q$ are the density and the velocity of the phase, respectively.

2.3. Momentum conservation

The two-phase flow model must guarantee the conservation of momentum as well.

The momentum balance for the generic phase q, without body forces, yields

$$\frac{\partial \mathbf{u}_q}{\partial t} + \mathbf{u}_q \cdot \nabla \mathbf{u}_q = \mathbf{F}_{p,q} + \mathbf{F}_{v,q} + \mathbf{F}_{d,q} \tag{5}$$

where $\mathbf{F}_{p,q}$ is representative of the pressure contribution, $\mathbf{F}_{v,q}$ of the viscous force, and $\mathbf{F}_{d,q}$ of the drag force, i.e. the interaction between the phases.

The pressure and the viscous force contribution are given by

$$\mathbf{F}_{p,q} = -\frac{1}{\rho_q} \nabla p \qquad \mathbf{F}_{v,q} = \frac{1}{\rho_q \alpha_q} \nabla \cdot (\alpha_q \bar{\bar{\tau}}_q) \tag{6}$$

where the stress tensor is written as

$$\bar{\bar{\tau}}_q = \mu_q (\nabla \mathbf{u}_q + \nabla \mathbf{u}_q^{\mathrm{T}}) \tag{7}$$

where μ_q is the shear viscosity and the superscript T denotes the transpose of $\nabla \mathbf{u}_q$.

Referring to the primary phase l and to the secondary phase g, the drag force [1, 7] can be written as

$$\mathbf{F}_{d,l} = \frac{3}{4} \frac{C_{\mathrm{D}}}{d_g \rho_l} \alpha_g \rho |\mathbf{u}_g - \mathbf{u}_l| (\mathbf{u}_g - \mathbf{u}_l) \tag{8}$$

$$\mathbf{F}_{d,g} = \frac{3}{4} \frac{C_{\mathrm{D}}}{d_g \rho_g} \alpha_l \rho |\mathbf{u}_l - \mathbf{u}_g| (\mathbf{u}_l - \mathbf{u}_g) \tag{9}$$

where C_{D} is the drag coefficient, d_g is the diameter of the bubbles of the secondary phase and ρ is the mixture density defined as

$$\rho = \alpha_l \rho_l + \alpha_g \rho_g \tag{10}$$

2.4. System of equations

Referring to the primary phase as l and to the secondary phase as g, the set of unknowns is given by the primitive variables

$$\boldsymbol{U} = (p \quad u_l \quad v_l \quad \alpha_g \quad u_g \quad v_g)^{\mathrm{T}} \tag{11}$$

Hence, the final system of equations consists of six equations: five equations are given by the conservation of the momentum for each phase and the continuity equation written for the

secondary phase volume fraction. The other continuity equation is not needed because of the costitutive relation (Equation (3)).

The sixth equation is obtained from the conservation of the total volume ($\sum_{q=l,g} \alpha_q = 1$) applied to the mass conservation equations. It reads

$$\sum_{q=l,g} \nabla \cdot (\alpha_q \mathbf{u}_q) = 0 \tag{12}$$

In this equation, the artificial compressibility formulation is used, i.e. a pressure time derivative is introduced to enhance robustness for steady state simulations [8]. Hence, the re-arranged equation for the pressure computation is

$$\frac{1}{\rho c^2} \frac{\partial p}{\partial t} + \nabla \cdot ((1-\alpha_g)\mathbf{u}_l) + \nabla \cdot (\alpha_g \mathbf{u}_g) = 0 \tag{13}$$

where c is a reference velocity and ρ is the mixture density.

3. FINITE ELEMENT APPROACH

The discretization of the governing equations is done through a Galerkin finite element approach with $P1$ basis functions for all the variables [9]. This means piecewise linear functions are used both for the basis and the weighting functions and the domain is discretized into triangles. In addition, a Petrov–Galerkin stabilization is employed.

3.1. Galerkin formulation

The governing equations can be written as a system of equations in terms of the chosen set of variables $\boldsymbol{U}$

$$\mathscr{L}(\boldsymbol{U}) = \boldsymbol{A}_0 \boldsymbol{U}_{,t} + \boldsymbol{F}^{\text{adv}}_{i,i} - \boldsymbol{F}^{\text{diff}}_{i,i} = \boldsymbol{S} \tag{14}$$

where $\boldsymbol{F}^{\text{adv}}_{i,i} = \boldsymbol{A}_i \boldsymbol{U}_{,i}$ is the advective contribution, $\boldsymbol{F}^{\text{diff}}_{i,i}$ is the diffusive (pressure and viscous term) contribution, and $\boldsymbol{S}$ represents the source term.

Introducing the trial solution space $\mathscr{V}_h$, and the weighting solution space $\mathscr{W}_h$, the weak form of (14) reads as find $\boldsymbol{U} \in \mathscr{V}_h$ such that $\forall\, \boldsymbol{W} \in \mathscr{W}_h$

$$\int_\Omega (\boldsymbol{W} \cdot \boldsymbol{A}_0 \boldsymbol{U}_{,t} + \boldsymbol{W} \cdot \boldsymbol{F}^{\text{adv}}_{i,i} + \boldsymbol{W}_{,i} \cdot \boldsymbol{F}^{\text{diff}}_i - \boldsymbol{W} \cdot \boldsymbol{S})\, \mathrm{d}\Omega$$
$$- \int_\Gamma (\boldsymbol{W} \cdot \boldsymbol{F}^{\text{diff}}_i)\, n_i\, \mathrm{d}\Gamma = 0 \tag{15}$$

where Ω is the spatial domain, Γ represents its boundaries and n_i is a component of the outer unit normal to the boundary.

3.2. SUPG formulation

The stabilization is obtained following a SUPG procedure applied to advection–diffusion systems. The new integral equation is

$$\int_\Omega (\boldsymbol{W}\cdot\boldsymbol{A}_0\boldsymbol{U}_{,t} + \boldsymbol{W}\cdot\boldsymbol{F}^{\text{adv}}_{i,i} + \boldsymbol{W}_{,i}\cdot\boldsymbol{F}^{\text{diff}}_i - \boldsymbol{W}\cdot\boldsymbol{S})\,\mathrm{d}\Omega - \int_\Gamma (\boldsymbol{W}\cdot\boldsymbol{F}^{\text{diff}}_i)\,n_i\,\mathrm{d}\Gamma + \boldsymbol{ST}_{\text{SUPG}} = 0 \tag{16}$$

where

$$\boldsymbol{ST}_{\text{SUPG}} = \sum_{e=1}^{n_{\text{el}}} \int_{\Omega_e} \boldsymbol{A}_i^{\text{T}}\boldsymbol{W}_{,i}\cdot\boldsymbol{\tau}(\mathscr{L}(\boldsymbol{U}) - \boldsymbol{S})\,\mathrm{d}\Omega \tag{17}$$

In the above formula Ω_e is one of the n_{el} elements in which the domain is divided, and $\boldsymbol{\tau}$ represents the matrix of the intrinsic time scales of the stabilizing operator.

The choice of $\boldsymbol{\tau}$ is cumbersome [10]. In this work a simple diagonal matrix is used

$$\boldsymbol{\tau} = \text{diag}(\tau_p, \tau_{ml}, \tau_{ml}, \tau_\alpha, \tau_{mg}, \tau_{mg}) \tag{18}$$

The values of the τ's are obtained by applying the one-dimensional theory to each equation. Specifically, the values available in the literature [5, 6, 9] are considered and re-arranged for this methodology.

In particular, the time scale for the secondary-phase momentum equation is chosen as

$$\tau_{mg} = \frac{\alpha_g h_g}{2\|\mathbf{u}_g\|}\zeta(Re^{h_g}) \tag{19}$$

where h is the element length in the direction of the local flow, $\mathbf{u}_g$ the local advection velocity, Re^{h_g} the element Reynolds number based on the element length and ζ a function of Re^{h_g}. Their definitions are

$$Re^{h_g} = \frac{h_g\|\mathbf{u}_g\|}{2\nu_g} \tag{20}$$

$$\zeta = \max\left[0, \min\left(\frac{Re^{h_g}}{3}, 1\right)\right] \tag{21}$$

$$h_g = \frac{2}{\sum_{i=1}^{3}\left|\dfrac{\mathbf{u}_g}{\|\mathbf{u}_g\|}\cdot\nabla\omega_i^{\mathbf{u}_g}\right|} \tag{22}$$

where the summation is performed for all the nodes of the element and $\omega_i^{\mathbf{u}_g}$ are the weighting functions associated to the secondary phase velocity.

Similarly, the time scale for the primary-phase momentum equation is chosen as

$$\tau_{ml} = \frac{(1-\alpha_g)h_l}{2\|\mathbf{u}_l\|}\zeta(Re^{h_l}) \tag{23}$$

with

$$Re^{h_l} = \frac{h_l \|\mathbf{u}_l\|}{2\nu_l} \tag{24}$$

$$h_l = \frac{2}{\sum_{i=1}^{3} \left| \frac{\mathbf{u}_l}{\|\mathbf{u}_l\|} \cdot \nabla \omega_i^{\mathbf{u}_l} \right|} \tag{25}$$

In this work, the evaluation of τ_p hs not been considered, since zero matrix entries correspond to the time scale related to the pressure equation residual in the SUPG framework. Finally, the expression of τ_α will be given in the next subsection.

3.3. Stabilization of the continuity equation

The key point of the proposed finite element approach concerns with the stabilization of the continuity equation.

Let us consider Equation (4) written in terms of α_g

$$\frac{\partial \alpha_g}{\partial t} + \mathbf{u}_g \cdot \nabla \alpha_g + (\nabla \cdot \mathbf{u}_g)\alpha_g = 0 \tag{26}$$

which is a scalar advection–reaction equation, where $\mathbf{u}_g$ is the advection velocity and $\nabla \cdot \mathbf{u}_g$ the reaction source. Then, the choice of the time scale τ_α follows the analogous choice of the scalar advection–reaction equation given in Reference [11]

$$\tau_\alpha = \frac{C_1}{\dfrac{2\|\mathbf{u}_g\|}{h_g} + C_2 |\nabla \cdot \mathbf{u}_g|} \tag{27}$$

where C_1 and C_2 are constants set through numerical tests. Suggested values, to prevent adding too much numerical viscosity, are $C_1 = 0.5$ and $C_2 = 12$.

Moreover, in order to prevent oscillations in the boundary layer region, a discontinuity capturing operator [5] is introduced for the continuity equation. The scalar weighting function referred to α_g is increased in the following way:

$$\tilde{\omega}_i^\alpha = \omega_i^\alpha + \tau_\alpha \mathbf{u}_g \cdot \nabla \omega_i^\alpha + \tau_{\alpha_2} \mathbf{u}_{g_\parallel} \cdot \nabla \omega_i^\alpha \tag{28}$$

with the last term representing the contribution coming from the discontinuity capturing operator. The definitions for $\mathbf{u}_{g_\parallel}$ and τ_{α_2} are

$$\mathbf{u}_{g_\parallel} = \begin{cases} \dfrac{(\mathbf{u}_g \cdot \nabla \alpha_g)}{\|\nabla \alpha_g\|^2} \nabla \alpha_g & \text{if } \nabla \alpha_g \neq 0 \\ 0 & \text{if } \nabla \alpha_g = 0 \end{cases} \tag{29}$$

and

$$\tau_{\alpha_2} = \max(0, \tau_{\alpha_\parallel} - \tau_\alpha) \tag{30}$$

with

$$\tau_{\alpha_{\|}} = \frac{C_1}{\dfrac{2\|\mathbf{u}_{g_{\|}}\|}{h_{g_{\|}}} + C_2|\nabla \cdot \mathbf{u}_g|} \tag{31}$$

From their definitions, $\mathbf{u}_{g_{\|}}$ is the component of $\mathbf{u}_g$ in the direction of the α_g gradient, and τ_{α_2} is the extra-amount of the time scale in the $\mathbf{u}_{g_{\|}}$ direction. In the above formulas, $h_{g_{\|}}$ is computed from $\mathbf{u}_{g_{\|}}$ and it is equal to

$$h_{g_{\|}} = \frac{2}{\sum_{i=1}^{3} \left| \dfrac{\mathbf{u}_{g_{\|}}}{\|\mathbf{u}_{g_{\|}}\|} \cdot \nabla \omega_i^{\mathbf{u}_g} \right|} \tag{32}$$

3.4. Time discretization technique

In this subsection the temporal discretization is briefly described. All the non-linear terms are treated explicitly in time, while the pressure and viscous terms (which are linear) implicitly. This choice leads us to discretize explicitly in time only non-linear terms, in order to finally obtain a linear system of equations to be solved with a biconjugate gradient solver.

Moreover, the schemes used for time discretization assure second-order accuracy in time for both, explicit and implicit, approaches. In fact, a Crank–Nicolson method is used for the pressure and diffusion terms, while an Adams–Bashforth method for all non-linear terms.

4. REMARKS ON THE STABILIZATION METHOD

In this section, further details of the stabilization technique are given. The main idea is to prove it acts consistently with a PSPG-SUPG stabilization *criterium* used for the incompressible NS equations, in the case P1 linear interpolation functions and Galerkin approach are employed, so successfully circumventing the so-called Babuśka–Brezzi (BB) condition [4, 12–14].

4.1. Navier–Stokes equations

The traditional stabilization method for a Galerkin finite element discretization of the incompressible NS equations is the so-called PSPG (Petrov–Galerkin pressure stabilization) stabilization for the continuity equation and SUPG stabilization for the momentum equation.

This method consists by adding the following stabilizing terms to the integral formulation of the continuity and momentum equations:

$$S_{\mathrm{PSPG}} = \sum_e \int_{\Omega_e} (\tau_{\mathrm{PSPG}} \nabla \omega_i^p) \cdot \mathbf{r}_{\mathrm{mom}}^h \, \mathrm{d}\Omega_e \tag{33}$$

$$S_{\mathrm{SUPG}} = \sum_e \int_{\Omega_e} \left(\tau_{\mathrm{SUPG}} \mathbf{u}^h \cdot \nabla \omega_i^{\mathbf{u}}\right) \mathbf{r}_{\mathrm{mom}}^h \, \mathrm{d}\Omega_e \tag{34}$$

where $\mathbf{r}_{\mathrm{mom}}^h$ is the residual of the discrete momentum equation, τ_{PSPG} and τ_{SUPG} are the appropriate PSPG and SUPG time scales, and ω_i^p and $\omega_i^{\mathbf{u}}$ are the weighting functions associated to the pressure and the velocity.

The same kind of stabilization is obtained when the SUPG formula (16) for a system of equations is applied to the NS equations. This is done by writing the equations in terms of the primitive variable and choosing the following $\boldsymbol{\tau}$ matrix:

$$\boldsymbol{\tau} = \mathrm{diag}(0, \tau_m, \tau_m) \tag{35}$$

with $\tau_{\mathrm{PSPG}} = \tau_{\mathrm{SUPG}} = \tau_m$.

4.2. *Two-fluid model*

In the present discretization, the SUPG term given in (17) is used. It depends from the Euler–Jacobian matrices $\boldsymbol{A}_i$, with $\boldsymbol{F}_{i,i}^{\mathrm{adv}} = \boldsymbol{A}_i \boldsymbol{U}_{,i}$.

The two matrices $\boldsymbol{A}_x$ and $\boldsymbol{A}_y$ specifically are

$$\boldsymbol{A}_x = \begin{pmatrix} 0 & 1-\alpha_g & 0 & u_g - u_l & \alpha_g & 0 \\ 0 & u_l & 0 & 0 & 0 & 0 \\ 0 & 0 & u_l & 0 & 0 & 0 \\ 0 & 0 & 0 & u_g & \alpha_g & 0 \\ 0 & 0 & 0 & 0 & u_g & 0 \\ 0 & 0 & 0 & 0 & 0 & u_g \end{pmatrix} \quad \boldsymbol{A}_y = \begin{pmatrix} 0 & 0 & 1-\alpha_g & v_g - v_l & 0 & \alpha_g \\ 0 & v_l & 0 & 0 & 0 & 0 \\ 0 & 0 & v_l & 0 & 0 & 0 \\ 0 & 0 & 0 & v_g & 0 & \alpha_g \\ 0 & 0 & 0 & 0 & v_g & 0 \\ 0 & 0 & 0 & 0 & 0 & v_g \end{pmatrix} \tag{36}$$

Introducing $\boldsymbol{A}_x$ and $\boldsymbol{A}_y$ in Equation (17), the stabilizing terms to be added to each equation are obtained.

In particular, the stabilizing term for the momentum equation of the generic phase q is equal to

$$S_{mq} = \sum_e \int_{\Omega_e} (\tau_{mq} \mathbf{u}_q{}^h \cdot \nabla \omega_i^{\mathbf{u}_q}) \mathbf{r}_{mq}^h \, \mathrm{d}\Omega_e \tag{37}$$

where $\mathbf{r}_{mq}^h$ is the residual of the discrete q-phase momentum equation. It is clear that the obtained stabilization term has the same expression as the one used in the momentum equation of the NS equations.

As far as the pressure equation concerns (13), the stabilizing term is

$$\begin{aligned} S_p = &\sum_e \int_{\Omega_e} (1-\alpha_g^h)(\tau_{ml} \nabla \omega_i^p) \cdot \mathbf{r}_{ml}^h \, \mathrm{d}\Omega_e + \sum_e \int_{\Omega_e} \alpha_g^h (\tau_{mg} \nabla \omega_i^p) \cdot \mathbf{r}_{mg}^h \, \mathrm{d}\Omega_e \\ &+ \sum_e \int_{\Omega_e} \tau_\alpha (\mathbf{u}_g^h - \mathbf{u}_l^h) \cdot \nabla \omega_i^p r_\alpha^h \, \mathrm{d}\Omega_e \end{aligned} \tag{38}$$

where $\mathbf{r}_{ml}^h$ is the residual of the discrete momentum equation of the primary phase, $\mathbf{r}_{mg}^h$ the residual of the discrete momentum equation of the secondary phase, and $\mathbf{r}_\alpha^h$ is the residual of the continuity equation for α_g. When the flow reduces to single-phase flow, $\alpha_g = 0$ and its residual vanishes, so that the stabilizing term is equal to the PSPG term in Equation (33).

5. NUMERICAL RESULTS

In this section, the results of the numerical simulation of the two-phase, laminar, steady flows in a channel and in a T-junction are presented.

5.1. *Two-phase flow in a channel*

The first test case concerns with the two-dimensional two-phase laminar flow in a channel. Nevertheless, this example presents a relatively simple geometry, the presence of the two phases renders the flow much more complex than the single-phase one. In the present computations, no interactions between the two phases are considered (i.e. zero drag force).

The simulation is done by giving the velocity at the inlet and setting uniform pressure at the outlet. The pressure at the inlet comes from the computation. The other boundaries are treated as no-slip walls. The chosen inlet velocity profile is set to be uniform. The geometry is shown in Figure 1.

The Reynolds number is defined as

$$Re = \frac{ud}{v} \tag{39}$$

where u is the inlet velocity and v is the kinematic viscosity. Table I shows the physical properties of the two phases.

Different grids are considered: the coarsest grid consists of 1699 nodes and 3236 elements, and the finest one consists of 33 965 nodes and 67 168 elements. The grids shows a boundary layer refinement.

The comparison with the results given in Reference [15] is done for the horizontal velocity profiles of both phases along the centre line of the channel. The results, as seen in Figure 2(a), show a quite good agreement with the reference solution. In Figure 2(b) the dependency of the solution from the grid is also shown.

Further comparisons are made for the pressure and the volume fraction. Figure 3(a) shows the static pressure along the centre line of the channel for the two different solutions. Regarding the volume fraction, the comparison is made through the values obtained along a vertical cut at $x = 2.5d$. The results are shown in Figure 3(b).

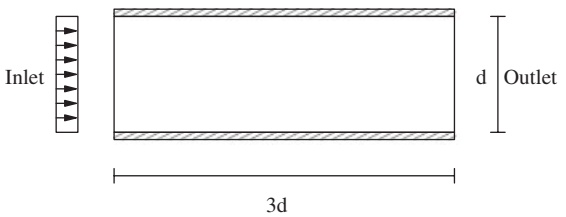

Figure 1. Two-phase flow in a channel—geometry.

Table I. Two-phase flow in a channel—physical properties.

Reynolds number	$Re_1 = 100$	$Re_2 = 100$
Kinematic viscosity	$\mu_1 = 0.01$	$\mu_2 = 0.005$
Density	$\rho_1 = 1.0$	$\rho_2 = 0.5$
Inlet volume fraction	$\alpha_1 = 0.5$	$\alpha_2 = 0.5$

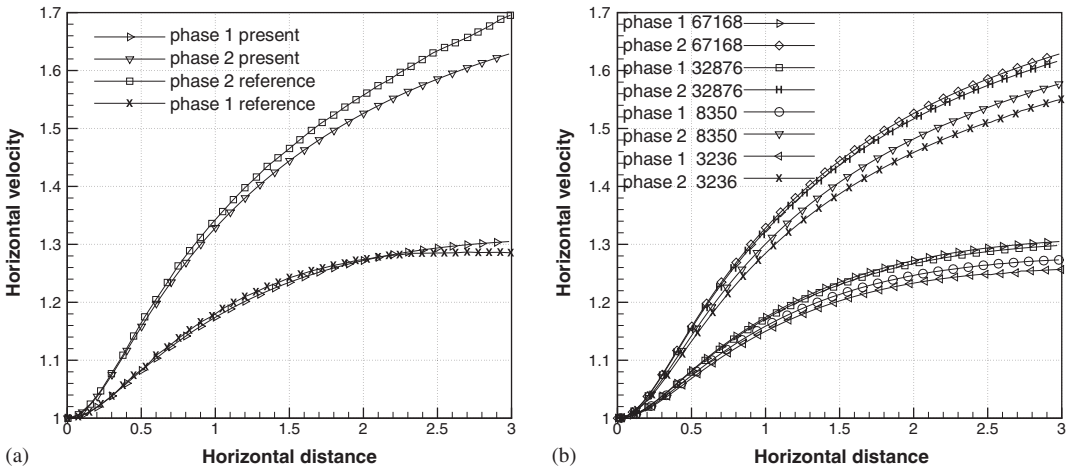

Figure 2. Two-phase flow in a channel—comparison for horizontal velocity profiles along $y = 0.5d$ between Reference [15] and the present solution (a), and with different grids (b).

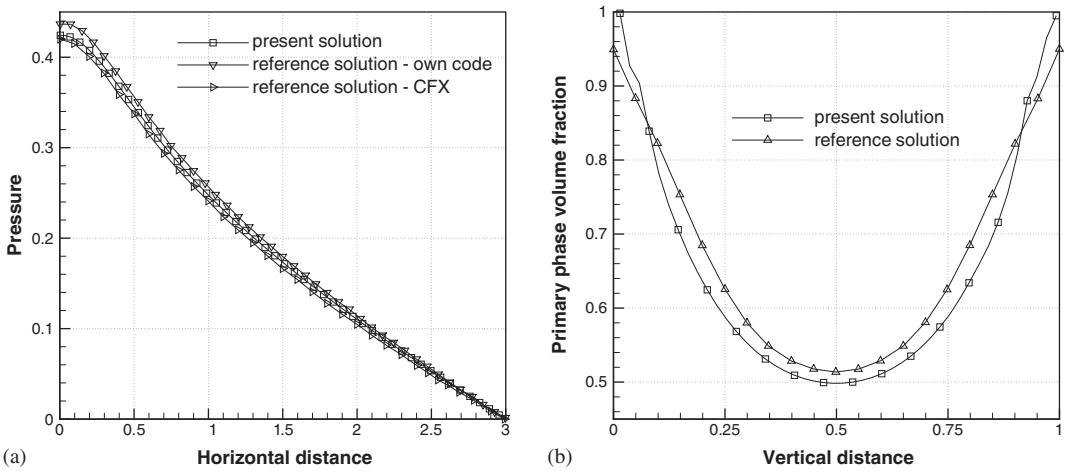

Figure 3. Two-phase flow in a channel—comparison between the present and the reference solution [15] for the pressure profiles along $y = 0.5d$ (a), and for the primary phase volume fraction profiles along $x = 2.5d$ (b).

5.2. *Two-phase flow in a T-junction*

The aim of this test case is to demonstrate the correctness of the implementation of the model and its accuracy for relatively complex flow patterns due to phase separation and mixing. The solution obtained is again compared with the one presented in Reference [15]. The geometry of the problem is shown in Figure 4.

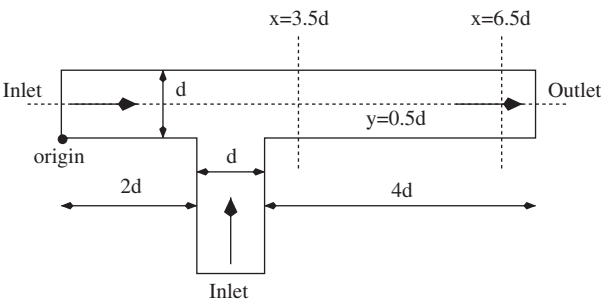

Figure 4. Two-phase flow in a T-junction—geometry of the problem.

Table II. Two-phase flow in a T-junction—physical properties.

Reynolds number	$Re_1 = 100$	$Re_2 = 75$
Kinematic viscosity	$\mu_1 = 0.01$	$\mu_2 = 0.0066$
Density	$\rho_1 = 1.0$	$\rho_2 = 0.5$
Inlet volume fraction	$\alpha_1 = 0.5$	$\alpha_2 = 0.5$

The simulation is carried out setting the same uniform velocity u at the two inlets and uniform pressure at the outlet. The remaining boundaries are treated as no-slip walls. Again the Reynolds number is defined as

$$Re = \frac{ud}{v} \tag{40}$$

On Table II the values of the physical properties of both phases are given.

Several unstructured grids are considered for the simulation. The coarsest grid consists of 1676 nodes and 3158 elements, and the finest one consists of 9981 nodes and 19 468 elements. The grids present a boundary layer refinement, to better reproduce the behaviour of the flow near the corners. In order to reproduce the results given in Reference [15], the same drag force parameters are used. In particular,

$$C_D = 1 \quad \text{and} \quad d_g = 0.1 \tag{41}$$

The comparison with the reference results [15] is carried out by plotting the horizontal and vertical velocity profiles along the centre line of the main channel of the T-junction. The results are shown in Figure 5(a). The velocity profiles are not referred to a specific phase. This is because the phases have the same components of the velocity, due to the presence of the drag force. Good agreement is achieved with the reference solution. In Figure 5(b) the grid dependency is also shown.

As far as the volume fraction concerns, the comparison is carried out at two different locations: $x = 3.5d$ and $x = 6.5d$. Figures 6(a) and (b) show the results of Reference [15] and the present solution. The agreement between the two solutions is less good respect to the one obtained for the velocity profiles. Nevertheless, the maximum value is still comparable. The major differences are located especially near the walls.

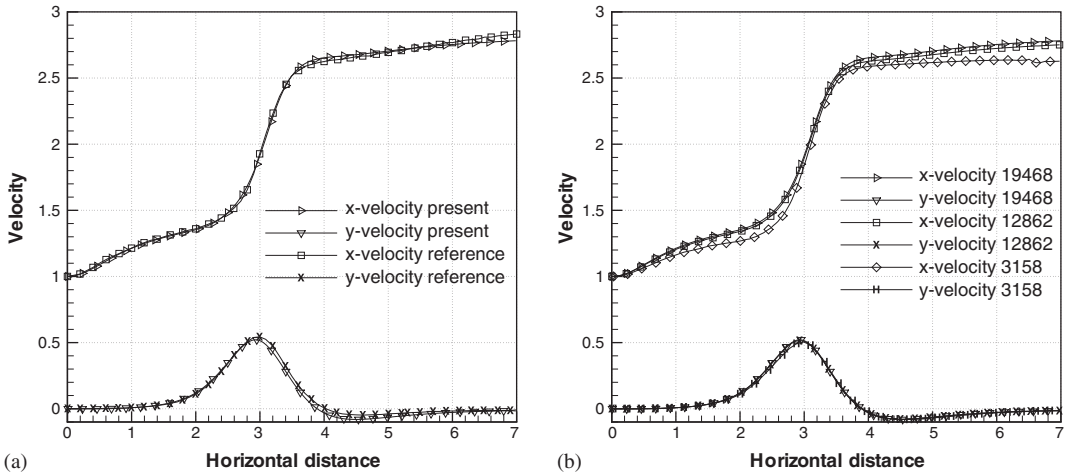

Figure 5. Two-phase flow in a T-junction—comparison for the velocity profiles along $y = 0.5d$ between Reference [15] and the present solution (a), and with different grids (b).

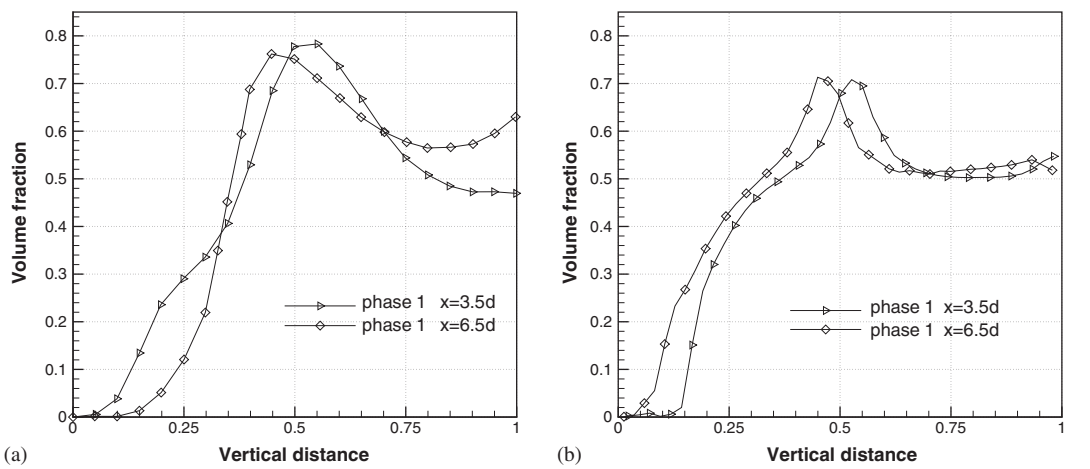

Figure 6. Two-phase flow in a T-junction—primary phase volume fraction profiles along $x = 3.5d$ and $x = 6.5d$: Reference [15] (a) and present solution (b).

6. CONCLUSIONS

In this paper a streamline upwind Petrov–Galerkin finite element formulation for two-phase flows has been shown.

The mathematical formulation of the two-phase flow model has been given and the strategy to achieve the discretization and the stabilization of the set of the resulting equations has been presented. The system of equations has been discretized as an advective–diffusive set of

equations and a SUPG stabilization has been performed by considering the advective matrix contributions. The accuracy of the method has been proved by comparing the results, in the case of multiple meshes, for the channel and the T-junction flow problems with the ones given in Reference [15].

The results highlight that the choice of this approach is very promising to simulate two-phase flows. The results also suggest that a better stabilization is needed in the boundary layer region, thus leading to the improvement of the discontinuity capturing operator acting in this region.

ACKNOWLEDGEMENTS

The authors gratefully acknowledge Prof H. Deconinck and Dr A. Bonfiglioli for their valuable contributions and suggestions. This work was partially supported by MIUR (Ministero dell'Istruzione, dell'Università e della Ricerca) under contract PRIN-2003 no. 2003092084_003.

REFERENCES

1. Ishii M. *Thermo-Fluid Dynamic Theory of Two-Phase Flow*. Eyrrolles: Paris, 1975.
2. Stewart HB, Wendroff B. Two-phase flow: models and methods. *Journal of Computational Physics* 1984; **56**:363–409.
3. Drew DA. Mathematical modeling of two-phase flow. *Annual Review on Fluid Mechanics* 1983; **15**:261–291.
4. Hughes TJR, Franca LP, Balestra M. A new finite element formulation for computational fluid dynamics: V. Circumventing the Babuska–Brezzi condition: a stable Petrov–Galerkin formulation of the Stokes problem accommodating equal-order interpolations. *Computer Methods in Applied Mechanics and Engineering* 1986; **59**:85–99.
5. Hughes TJR, Mallet M, Mizukami A. A new finite element formulation for computational fluid dynamics: II. Beyond SUPG. *Computer Methods in Applied Mechanics and Engineering* 1986; **54**:341–355.
6. Mizukami A. An implementation of the Streamline-Upwind/Petrov–Galerkin method for linear triangular elements. *Computer Methods in Applied Mechanics and Engineering* 1985; **49**(3):357–364.
7. Oliveira PJ, Issa RI. Numerical aspects of an algorithm for the Eulerian simulation of two-phase flow. *International Journal for Numerical Methods in Fluids* 2003; **43**:1177–1198.
8. Chorin AJ. A numerical method for solving incompressible viscous flow problems. *Journal of Computational Physics* 1967; **2**:12–26.
9. Tezduyar TE, Mittal S, Ray SE, Shih R. Incompressible flow computations with bilinear and linear equal-order interpolation velocity–pressure elements. *Computer Methods in Applied Mechanics and Engineering* 1992; **95**:221–242.
10. Hauke G, Hughes TJR. A comparative study of different sets of variable for solving compressible and incompressible flows. *Computer Methods in Applied Mechanics and Engineering* 1988; **153**:1–44.
11. Codina R. On stabilized finite element methods for linear systems of convection–diffusion–reaction equations. *Computer Methods in Applied Mechanics and Engineering* 2000; **188**:61–88.
12. Babuśka I. Error bounds for finite element methods. *Numerische Mathematik* 1971; **16**:322–333.
13. Babuśka I. The finite element method with Lagrangian multipliers. *Numerische Mathematik* 1973; **20**:179–192.
14. Brezzi F. On the existence, uniqueness and approximation of saddle-point problems arising from Lagrange multipliers. *R.A.I.R.O., Série Rouge Analyse Numérique* 1974; **8**(R-2):129–151.
15. Thompson CP, Lezeau P. A novel solution algorithm for incompressible, multi-phase viscous flows. *International Journal for Numerical Methods in Fluids* 1998; **28**:1217–1239.

